JOURNAL OF SOLID STATE CHEMISTRY **131,** 246–251 (1997)
ARTICLE NO. SC977368

Structural Characterization of Electrochemically Oxidized $La_2CuO_{4+\delta}$ Particles Prepared by a Sol–Gel Method

José Mahía,* José Luis Martínez-Lorenzo,† M. Carmen Blanco,† and M. Arturo López-Quintela†

**Servicios Xerais de Apoio á Investigación, Campus da Zapateira s/n, Universidade de A Coruña, E-15071 A Coruña, Spain; and*
†Depto. Química-Física, Facultade de Química, Av das Ciencias s/n, Universidade de Santiago de Compostela, E-15706 Santiago de Compostela, Spain

Received July 26, 1996; in revised form February 26, 1997; accepted March 3, 1997

The structure of powder samples of electrochemically oxidized $La_2CuO_{4+\delta}$ was studied using X-ray powder diffraction. The base La_2CuO_4 material was prepared by a sol–gel method that allowed control of the mean particle size by calcining at different temperatures. The results show that the structure of the electrochemically oxidized samples is very sensitive to the synthesis method, particularly the calcination temperature, T_{cal}. The refined lattice parameters *b* and *c*, the unit cell volume *V*, and the orthorhombicity of the oxidized samples are found to increase considerably when T_{cal} decreases. These variations indicate an increase in the quantity of interstitial oxygen in the samples calcined at lower temperatures with respect to the interstitial oxygen presents in ceramic samples. Particle size distributions were determined by transmission electron microscopy. A decrease in the mean particle size when T_{cal} decreases was observed. © 1997 Academic Press

INTRODUCTION

The family of cuprate superconductors based on the tetragonal K_2NiF_4 structure (*I*4/*mmm* space group) has remained of central interest for the understanding of the properties of these compounds due to their relatively simple structure (1–3). The intimate correlations between structure, doping, and superconducting properties are among the most important issues of interest in these materials. The prototype parent compound La_2CuO_4 has been widely studied (4, 5). La_2CuO_4 has the K_2NiF_4-type (T-phase) structure containing edge-squared CuO_6 octahedra arranged in a planar array above a given temperature T_t. The structure becomes orthorhombic (*Cmca* space groups) at $T < T_t$, due to the cooperative rotation of the CuO_6 octahedra that produces a compressive stress on the CuO_2 sheets that is caused by a mismatch of the equilibrium La–O bond length in the La_2O_2 layers and the Cu–O bond length of the CuO_2 sheets. It itself is an antiferromagnetic insulator, but it can be converted to a superconductor at ≈ 40 K, either by partial M(II) substitution in the La(III) sites (6, 7) or by insertion of additional oxygen into interstitial positions. The latter can be achieved by annealing the base material at high temperatures ($\approx 500°C$) in high oxygen partial pressure (8, 9) or by a simple anodic oxidation of the undoped compound in an aqueous KOH solution at room temperature (10–13).

The amount, nature, and location of interstitial oxygen has been subject of an interesting controversy (14–17). X-ray powder diffraction studies have revealed a structural evolution with δ in samples oxidized by the electrochemical method. At room temperature, the orthorhombic distortion (*Cmca* space group) decreases with increasing δ over the compositional range $0 \leq \delta \leq 0.05$. In the range $0.05 \leq \delta \leq 0.09$ a second orthorhombic distortion of higher symmetry (*Fmmm* space group) appears, increasing with δ.

The *c* lattice parameter increases continuously with increasing oxygen content (18). This elongation is the net result of an expansion of the LaO interlayer distance in the *z* direction, consistent with the introduction of interstitial oxygen between the LaO layers (19). The *b* lattice parameter and the orthorhombic strain has a pronounced minimum for $\delta \approx 0.05$ (20).

In this paper, we report the synthesis of La_2CuO_4 powders by a sol–gel method, which allows us to obtain single-phase materials even when the samples are calcined at temperatures as low as 600°C. We present the structural X-ray characterization of $La_2CuO_{4+\delta}$ samples obtained by electrochemical oxidation of the base compound, which allows us to gain insight into the oxygen stoichiometry of those compounds.

EXPERIMENTAL PROCEDURE

La_2CuO_4 base materials were prepared by a sol–gel reaction in an aqueous solution of stoichiometric amounts of La(III) and Cu(II) nitrates in the presence of urea. All the chemicals employed in this work were reagent grade (Aldrich, Steinheim, Germany) and were used without further purification. The initial concentrations were 0.2 M in

0022-4596/97 $25.00

La(III), 0.1 *M* in Cu(II), and 3 *M* in urea. The volume of the initial solution was 100 mL and it had blue color. The water of this solution was evaporated on a hot-plate at 75°C with continuous stirring and a gel formed upon cooling. This gel was decomposed in an oven at 250°C to yield the sample precursor, which was dry-ground for 30 min in a ball mill, heated at one of eight different temperatures between 600 and 950°C in order to obtain samples with different mean particle size and then again ground for 1 h. Calcination time was 6 h for all the samples, except for the sample calcined at 600°C, which needed 8 h to achieve a single-phase material, according to X-ray diffraction measurements. The calcination of the samples was carried out in a Quastar HEM·L·1 furnace in a static air atmosphere with a heating rate of 10°C/min. All the samples were cooled to room temperature in the furnace after calcination.

Another La_2CuO_4 sample for use as a polycrystalline reference was synthesized by a standard solid state reaction. For that purpose, a stoichiometric mixture of La_2O_3 and CuO was dry-ground in a ball mill for 30 min and then calcined in air successively at 950 and 1000°C for 12 and 20 h, respectively, and air quenched. The mixture was then reground and sintered at 1050°C for 24 h, and it was cooled to room temperature in the furnace after the annealing. The final product was a single-phase material free from impurity phases according to X-ray diffraction measurements.

Oxidation of the samples was carried out at room temperature under galvanostatic conditions. The electrochemical device consists of three electrodes in a cell filled with a 1 *M* KOH aqueous solution. The working electrode was a disk-shape pellet of the sample (13 mm ∅; 2 mm thick) made from the powder, and a platinum wire was embedded in it for electrochemical contact. The sample was sintered after pressed. As reference electrode a Ag/AgCl electrode was used; all potentials quoted in this work are referred to this electrode. A platinum counter electrode was used. A constant anodic current of 0.25 mA was applied to the sample working electrode, according to voltametric measurements previously carried out. The electrochemical oxidation was carried out for 72 h for each sample. The potential increased nearly continuously from a starting value of $\approx$0.3 to $\approx$0.6 V, in a few hours. When the potential reached the latter value, it remained practically constant for $\approx$60 h, to assure the electrochemical oxidation was completed. The final product was ground and dried in vacuum at room temperature overnight.

The polycrystalline powders obtained above were characterized by inductively coupled plasma atomic emission spectroscopy (ICP-AES), using a Perkin–Elmer 5000 with Ar plasma. For these measurements, samples were prepared dissolving $\approx$10 mg of each sample in 5 mL of HCl:HNO_3 (1:1) adding water until 100 mL. The concentration of each element was obtained as an average of three measurements. The structural characterization was carried out by X-ray powder diffraction (XRD), using a Philips PW-1710 diffractometer fitted with a Cu anode (Cu$K\alpha_1$ radiation, $\lambda = 1.54060$ Å; and Cu$K\alpha_2$ radiation, $\lambda = 1.54439$ Å; intensity ratio [Cu$K\alpha_1$/Cu$K\alpha_2$] $= 0.5$). Measurements were performed at room temperature between 20° and 100° (2Θ), with a step size of 0.005° and a step time of 2.5 s. The Rietveld method was used to derive refined lattice parameters from the XRD. Particle size distributions were determined by TEM in a Philips CM12 microscope. Samples were prepared by dry-grinding the cuprates in a ball mill for 1 h to separate the particles, dispersing them in water by using ultrasounds, and then immersing a copper grid coated with polyvinyl formal in the dispersion to fix the particles to it. At least 20 isolated particles were examined for each sample.

RESULTS AND DISCUSSION

Results of ICP measurements for the samples prepared both by solid state reaction and by the sol–gel method show a molar ratio La/Cu of 1.95 ± 0.10, demonstrating that the stoichiometry of the starting solutions is maintained in the final samples.

The powder diffractogram for La_2CuO_4 prepared by the sol–gel reaction and calcined at 600°C is shown in Fig. 1a.

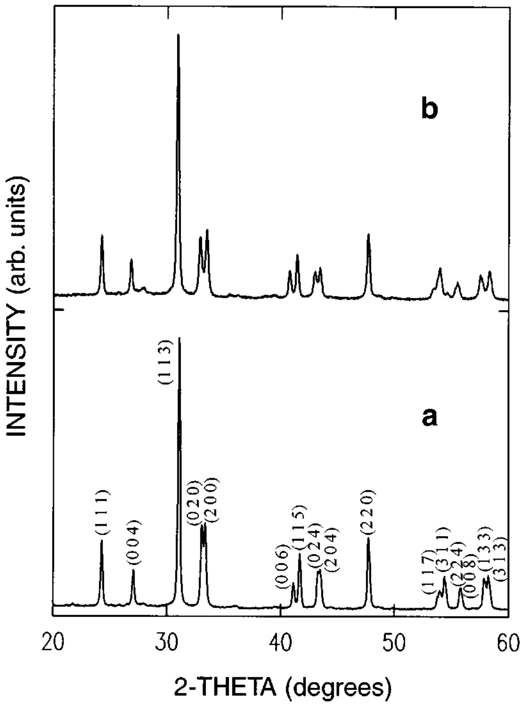

FIG. 1. X-ray diffractograms for the sample prepared by the sol–gel method and calcined at 600°C before (a) and after (b) oxidation.

TABLE 1
Lattice Parameters, Unit Cell Volume V, and Orthorhombicity for La_2CuO_4 Samples before Oxidation

T_{cal} (°C)	a (Å)	b (Å)	c(Å)	V (Å^3)	O%
Ceramic sample	5.3557(1)	5.4054(1)	13.1456(2)	380.56(2)	0.92
950	5.3565(1)	5.4047(1)	13.1525(2)	380.77(2)	0.89
900	5.3575(1)	5.4046(1)	13.1533(1)	380.86(1)	0.87
850	5.35748(1)	5.4053(1)	13.1510(1)	380.83(1)	0.89
800	5.3576(1)	5.4053(1)	13.1482(1)	380.83(1)	0.89
750	5.3582(1)	5.4051(1)	13.1497(2)	380.83(2)	0.87
700	5.3591(1)	5.4052(1)	13.1516(2)	380.96(2)	0.86
650	5.3592(1)	5.4055(1)	13.1506(2)	380.96(2)	0.86
600	5.3586(1)	5.4050(1)	13.1495(2)	380.85(2)	0.86

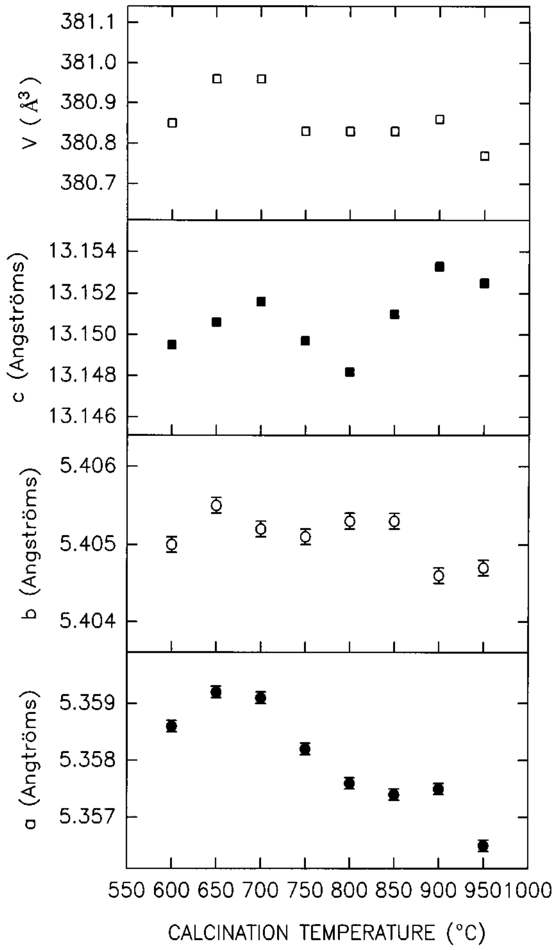

FIG. 2. Variation of the lattice parameters and the unit cell volume V with T_{cal} for the La_2CuO_4 samples prepared by the sol–gel method before the oxidation process.

The absence of peaks of secondary phases indicates that only 8 h heating at 600°C is necessary to prepare a pure La_2CuO_4 single-phase using this sol–gel method. The diffractograms for all the sol–gel samples were quite similar, but close examination revealed that the peak resolution was poorer for samples calcined at low temperatures, which may be associated with the broadening of the peaks due to the smaller grain size of the samples prepared at lower calcination temperatures, T_{cal}.

Table 1 gives the lattice parameters (*Cmca* space group; group No. 64) for La_2CuO_4 samples. Figure 2 shows the variation of the lattice parameters and the unit cell volume V, with T_{cal}. It can be seen that there is not a clear evolution of the lattice parameters with T_{cal}, contrary to the results obtained for the T′-R_2CuO_4 compounds (21), where lattice parameters increased with decreasing T_{cal}. The orthorhombicity of the samples O, defined by the relation $[2 \cdot (b - a)/(a + b)]$, is also practically independent of T_{cal} in the undoped samples.

X-ray diffractograms of the oxidized samples (Fig. 1b for the sample calcined at 600°C) show monophasic and well-crystallized powders, but there is a significant orthorhombic variation compared to the base sample. The oxidized samples have a more pronounced splitting of pairs of peaks ($h\,k\,l$) and ($k\,h\,l$). The orthorhombic (020–200) reflection peaks are shown in Fig. 3 and Fig. 4 for the samples prepared by the sol–gel reaction and calcined at 950 and 600°C, respectively, before and after oxidation. This variation suggests an enhanced orthorhombic distortion, as originally reported (22). Nevertheless the splitting is much larger in the oxidized sample calcined at 600°C than in the oxidized sample calcined at 950°C.

Crystal structure refinement of the oxidized sample prepared by the solid state reaction indicates that there is a significant increase of the c parameter (from 13.1456(2) to 13.2196(3) Å) and of the unit cell volume, while the a and b axes undergo a minor decrease and increase, respectively. These results are consistent with data reported previously (7, 20). The lattice parameters and the orthorhombicity of all the oxidized samples prepared by the sol–gel method are summarized in Table 2. Notice that there are very important differences in the lattice parameters of the oxidized samples as a function of the T_{cal} employed in the sol–gel method. The lattice parameters of the oxidized sol–gel samples calcined at 950°C are similar to those of the oxidized samples prepared by solid state reaction. However, when T_{cal} decreases the c axis increases considerably in the oxidized samples (Fig. 5) from 13,2205(2) Å for the sample calcined at 950°C to 13,2529(3) Å for the sample calcined at 600°C, which means ≈0.25% large in this temperature range. The b parameter also increases when T_{cal} decreases and the relative variation is even much larger than for the c axis: ≈0.32% in the same temperature range. The value of the a parameter undergoes a small decrease but there is not a monotonic variation with T_{cal}, as shown in Fig. 5 for the a axis. The unit cell volume V also increases when T_{cal}

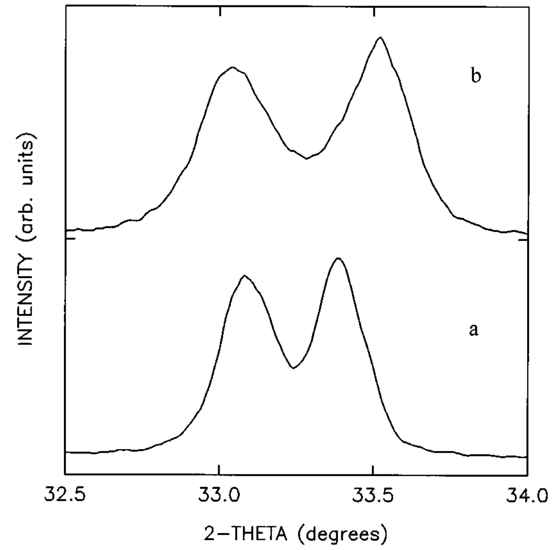

FIG. 3. (0 2 0) and (2 0 0) peaks for the sample prepared by the sol–gel method and calcined at 950°C before (a) and after (b) oxidation.

TABLE 2
Lattice Parameters, Unit Cell Volume *V*, and Orthorhombicity for Oxidized La_2CuO_4 Samples

T_{cal} (°C)	*a* (Å)	*b* (Å)	*c* (Å)	*V* (Å^3)	O%
Ceramic sample	5.3415(1)	5.4109(1)	13.2196(3)	382.08(3)	1.29
950	5.3415(1)	5.4130(1)	13.2205(2)	382.25(2)	1.33
900	5.3422(1)	5.4130(1)	13.2237(2)	382.39(2)	1.32
850	5.3436(1)	5.4174(1)	13.2282(3)	382.94(3)	1.37
800	5.3407(1)	5.4201(1)	13.2349(2)	383.11(2)	1.48
750	5.3386(1)	5.4219(1)	13.2357(3)	383.11(2)	1.55
700	5.3390(1)	5.4251(1)	13.2423(2)	383.56(2)	1.60
650	5.3398(1)	5.4282(1)	13.2480(3)	384.00(2)	1.64
600	5.3395(2)	5.4286(2)	13.2495(4)	384.05(2)	1.65

Comparing the lattice parameters of the oxidized samples calcined at 600°C with the as prepared samples before oxidation, it can be seen that there is a significant increase in the *c* axis (≈0.79%). The *b*-axis also increases but only by decreases. The volume change is ≈0.55% in the studied temperature range. The orthorhombicity of the oxidized samples also shows a significant variation with T_{cal}, as shown in Fig. 6. The value of O increases from 1.33% for the oxidized sample calcined at 950°C to 1.67% for the sample calcined at 600°C, which means an increment of ca. 25%. This result agrees with the larger splitting observed in the X-ray diffractogram of the sample calcined at 600°C.

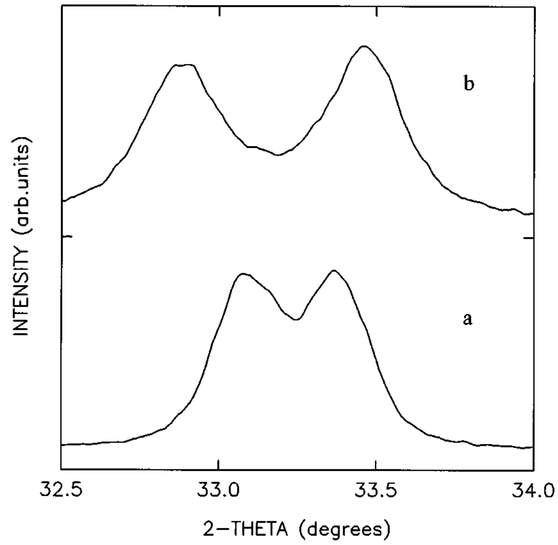

FIG. 4. (0 2 0) and (2 0 0) peaks for the sample prepared by the sol–gel method and calcined at 600°C before (a) and after (b) oxidation.

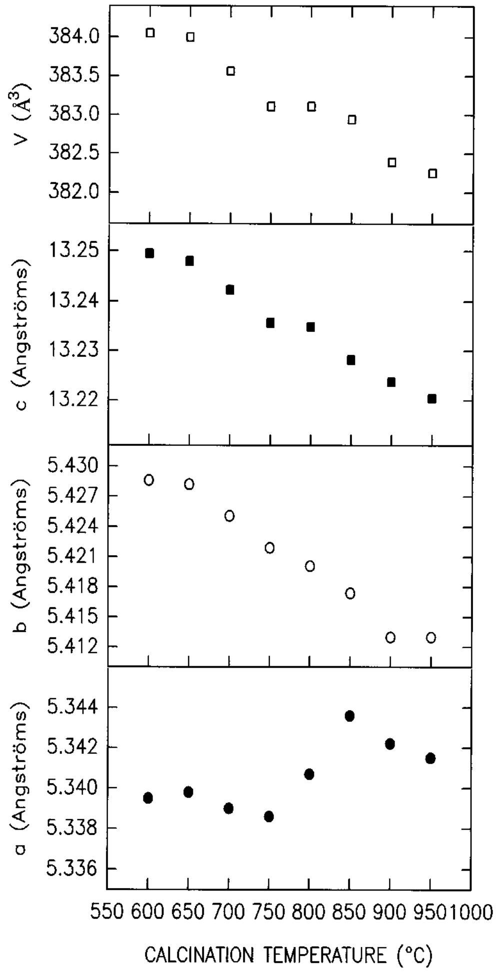

FIG. 5. Variation of the lattice parameters and the unit cell volume *V* with T_{cal} for the oxidized $La_2CuO_{4+\delta}$ samples prepared by the sol–gel method.

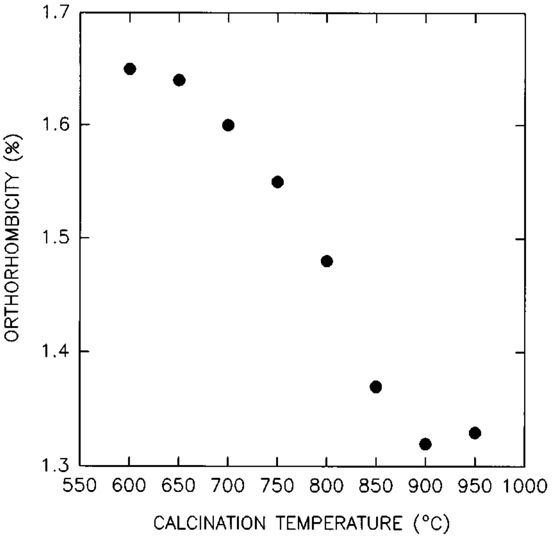

FIG. 6. Variation of the orthorhombicity with T_{cal} for the oxidized $La_2CuO_{4+\delta}$ samples prepared by the sol–gel method.

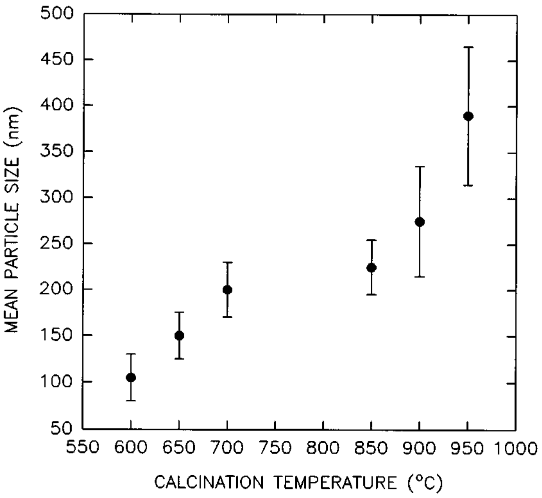

FIG. 7. Mean particle size vs T_{cal} obtained by TEM for La_2CuO_4 samples prepared by the sol–gel method.

≈0.47%, while the *a* axis shows an important decrease of ≈0.34%. These variations mean that the *b* and *c* parameters increase much more in the sample calcined at 600°C than in the samples prepared by solid state reaction ($\Delta c/c = +0.56\%$; $\Delta b/b = +0.10\%$).

The observed increase in the orthorhombicity and the larger values for the *b* and *c* lattice parameters in the oxidized samples calcined at lower temperatures seem to indicate a larger quantity of interstitial oxygen when T_{cal} decreases. This increase in the lattice parameters would be the result of an increase in the distance between the LaO layers through the *z* direction, due to the introduction of a larger quantity of interstitial oxygen in the LaO planes. On the other hand, this excess in the quantity of interstitial oxygen of the sol–gel samples calcined at low temperature should not short the Cu–O bond distance, so the *b* lattice parameter increases its value.

To check the increase in the oxygen stoichiometry after oxidation, a thermogravimetric analysis (TGA) in N_2 gas was carried out. A similar weight loss (≈0.7%) between 250 and 550°C is observed for the ceramic sample and the sol–gel one calcined at 950°C. Nevertheless, the weight loss of the sol–gel sample calcined at 600°C (1.9% in the 200–550°C range) is significantly larger as compared with the previous samples. The lost product in the TGA process was passed through a carbon layer and then analyzed by infrared spectroscopy (IR). We observed the CO characteristic bands in the IR diagram, proving that the weight decrease observed in the TGA experiments is due to an oxygen loss. The larger values of the orthorhombicity and the TGA weight loss indicate that the quantity of interstitial oxygen increases when the calcination temperature employed in the sol–gel synthesis process decreases.

The reason the samples calcined at low temperatures admit more interstitial oxygen could be related with the influence of the thermal treatment effect on the structure of the compound. The porosity of the sample increases when T_{cal} decreases due to the minor energy furnished with the calcination process and the structure then becomes more "soft" at low calcination temperatures (23). The interstitial oxygen atoms find less difficulties to be introduced in this soft structure during the electrochemical process, as the structure is able to adjust itself to new stoichiometry. The porosity of the lattice will then limit the admittance of interstitial oxygen in the compound.

Mean particle size of the samples was determined by TEM, and its variation with T_{cal} is shown in Fig. 7 for the undoped La_2CuO_4 samples prepared by the sol–gel method. For the samples studied here, mean particle size was found to increase with T_{cal}, from 100 ± 25 nm at 600°C to 400 ± 75 nm at 950°C (Fig. 8), but sizes are always smaller than the values reached for La_2CuO_4 prepared by the solid state reaction (≈1 μm). It was observed that the mean particle size of the oxidized samples does not vary with the electrochemical oxidation process. Comparing the variations of the lattice parameters of the oxidized samples and mean particle size with T_{cal}, it is seen that the latter decreases as the former increases. The above mentioned changes in the structure of the oxidized samples could then be related to the decreasing particle size.

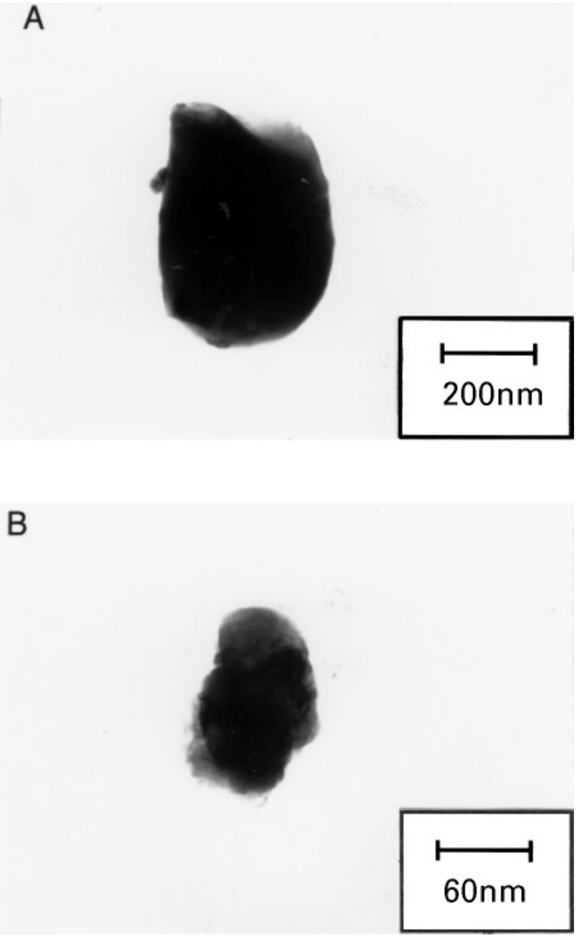

FIG. 8. TEM photographs for two La_2CuO_4 samples prepared by the sol–gel method and calcining at 950°C (A) and 600°C (B).

CONCLUSIONS

Preparation of La_2CuO_4 by the sol–gel method allows control of the mean particle size by changing T_{cal}. The calcination temperature employed in the sol–gel process has also an important influence on the oxygen stoichiometry and on the structure of the oxidized samples obtained by electrochemical oxidation at room temperature. The quantity of interstitial oxygen atoms increases considerably when T_{cal} decreases, as can be concluded by the large values obtained for the b and c parameters, and for the orthorhombicity of the oxidized samples calcined at low temperatures, as compared with those obtained for oxidized samples prepared by conventional techniques. TGA experiments confirm the interstitial oxygen excess in these samples. Oxidized samples prepared by a standard solid state reaction have a larger particle size and have a smaller quantity of interstitial oxygen than those prepared by the sol–gel method. The larger quantity of interstitial oxygen in the $La_2CuO_{4+\delta}$ samples opens a wide field of study of the influence of this new range of oxygen stoichiometry for this compound on superconductor properties.

ACKNOWLEDGMENTS

We are grateful to the Xunta de Galicia for financial support (Project XUGA 20902A93).

REFERENCES

1. J. G. Bednorz and K. A. Müller, *Z. Phys. B* **65,** 189 (1986).
2. F. C. Chou, J. H. Cho, L. L. Miller, and D. C. Johnson, *Phys. Rev. B* **42,** 6172 (1990).
3. J. B. Goodenough, J.-S. Zhou, and J. Chan, *Phys. Rev. B* **47,** 5275 (1993).
4. Von B. Grande, Hk. Müller-Buschbaum, and M. Schweizer, *Z. Anorg. Allg. Chem.* **428,** 120 (1977).
5. S-W. Cheong, J. D. Thompson, and Z. Fisk, *Physica C* **158,** 109 (1989).
6. J. M. Tarascon, L. H. Greene, W. R. MacKinnon, G. W. Hull, and T. H. Geballe, *Science* **235,** 1373 (1987).
7. F. C. Chou, J. H. Cho, and D. C. Johnston, *Physica C* **197,** 303 (1992).
8. J. Beille, B. Chevalier, G. Demazeau, F. Deslandes, J. Etourneau, O. Laborde, C. Michel, P. Lejay, J. Provost, B. Raveau, A. Sulpice, J. L. Tholence, and R. Tournier, *Physica B* **146,** 307 (1987).
9. J. E. Schirber, B. Morosin, R. M. Merrill, P. F. Hlava, E. L. Venturini, J. F. Kwak, P. J. Nigrey, R. J. Baughman, and D. S. Ginley, *Physica C* **152,** 121 (1988).
10. A. Wattiaux, J. C. Park, J. C. Grenier, and M. Pouchard, *C.R. Acad. Sci. Paris* **310,** 1047 (1990).
11. P. G. Radaelli, J. D. Jorgensen, A. J. Schultz, B. A. Hunter, J. L. Wagner, F. C. Chou, and D. C. Johnston, *Phys. Rev. B* **48,** 499 (1993).
12. R. Suryanarayanan, O. Gorochov, M. S. R. Rao, L Ouhammou, W. Paulus, and G. Heger, *Physica C* **185–189,** 573 (1991).
13. G. Rajaram, R. Suryanarayanan, N. LeNagard, O. Gorochcv, L. Ouhammou, W. Paulus, and G. Heger, *Physica C* **199,** 139 (1992).
14. C. Chaillout, S. W. Cheong, Z. Fisk, M. S. Lehmann, M. Marezio, B. Morosin, and J. E. Schirber, *Physica C* **158,** 183 (1989).
15. C. Chaillout, J. Chenavas, S. W. Cheong, Z. Fisk, M. Marezio, B. Morosin, and J. E. Schirber, *Physica C* **170,** 87 (1990).
16. J. Ryder, P. A. Midgley, P. Exley, R. J. Beynon, D. L. Yates, L. Afalfiz, and J. A. Wilson, *Physica C* **173,** 9 (1991).
17. J. D. Jorgensen, B. Dabrowski, Shiyou Pei, D. G. Hinks, L. Soderholm, B. Morosin, J. E. Schirber, E. L. Venturini, and D. S. Ginley, *Phys. Rev. B* **38,** 11337 (1988).
18. P. Rudolf, W. Paulus, and R. Schöllhorn, *Adv. Mater.* **3,** 438 (1991).
19. J.-C. Grenier, N. Lagueyte, A. Wattiaux, J-P. Doumerc, P. Dordor, J. Etourneau, M. Pouchard, J. B. Goodneough, and J. S. Zhou, *Physica C* **202,** 209 (1992).
20. N. Lagueyte, A. Wattiaux, J. C. Park, J.-C. Grenier, L. Fournès, and M. Pouchard, *J. Phys. III* **1,** 1755 (1991).
21. J. Mahia, A. Vieiro, J. Mira, J. Rivas, A. López-Quintela, and S. B. Oseroff, *J. Solid State Chem.* **122,** 25 (1996).
22. J.-C. Grenier, A. Wattiaux, N. Lagueyte, J. C. Park, E. Marquestaut, J. Etourneau, and M. Pouchard, *Physica C* **173,** 139 (1991).
23. J. M. Reed, *in* "Introduction to the Principles of Ceramic Processing." Wiley, New York, 1988.